

MICROSTRUCTURE EVOLUTION AND ELECTRICAL PROPERTIES OF $\text{Ba}_2\text{NaNb}_5\text{O}_{15}$ AND BaTiO_3 COMPOSITES

MYOUNG-SUP KIM, JOON-HYUNG LEE, JEONG-JOO KIM, HEE YOUNG LEE*, SANG-HEE CHO

Department of Inorganic Materials Engineering, Kyungpook National University, Daegu 702-701, Korea

*Department of Materials Science and Engineering, Yeungnam University, Gyeongsan 712-749, Korea

E-mail: jjkim@knu.ac.kr

Submitted September 17, 2004; accepted December 12, 2004

Keywords: Ferroelectrics, Composite, BNN-BT, Sintering, Dielectric characteristics

Phase development and sintering behavior and dielectric characteristics of the composites of tungsten bronze structured $\text{Ba}_2\text{NaNb}_5\text{O}_{15}$ (BNN) and perovskite structured BaTiO_3 (BT) were examined as a function of molar ratio x in $(1-x)\text{Ba}_2\text{NaNb}_5\text{O}_{15}-x\text{BaTiO}_3$. A wide range of solid solution of BT in BNN was observed up to $x=0.4-0.6$, and the lattice constants increased with BT contents. Since the solid solution of BT expelled Na ions from BNN, liquid phase with excess Na might be produced during sintering and resulted in accelerated densification and abnormal grain growth. More BT addition in BNN over the solubility limit produced a second phase of $\text{Ba}_6\text{Ti}_7\text{Nb}_9\text{O}_{40}$ together with BT, and those phases played a role as grain growth inhibitors. The Curie temperature (TC) and the maximum dielectric constant of BNN decreased as the content of BT increased. Besides, when BNN is added to BT, the solubility limit of BNN in BT was very narrow compared to the case of BT addition to BNN, which resulted in the generation of $\text{Ba}_6\text{Ti}_7\text{Nb}_9\text{O}_{40}$ second phase. The addition of BT to BNN also shifted the TC to lower temperature. In the case of $x=0.6$, two dielectric relaxation peaks were observed which is believed due to the coexistence of BNN and BT in the sample.

INTRODUCTION

The perovskite is one of the most representative crystal structures among various ferroelectric materials. BaTiO_3 , PbTiO_3 , $\text{Pb}(\text{Zr}_x\text{Ti}_{1-x})\text{O}_3$, $\text{Pb}(\text{Mg}_{1/3}\text{Nb}_{2/3})\text{O}_3$, etc. have the typical perovskite structure of ABO_3 . Another well known crystal structure showing ferroelectric characteristics is of tungsten bronze. $\text{Sr}_x\text{Ba}_{1-x}\text{Nb}_2\text{O}_6$ (SBN), $\text{Ba}_2\text{NaNb}_5\text{O}_{15}$ (BNN), $\text{K}_3\text{Li}_2\text{Nb}_5\text{O}_{15}$ (KLN) are the typical materials of tungsten bronze structure with the unit cell formula of $[(\text{A}1)_2(\text{A}2)_4]\text{C}_4[(\text{B}1)_2(\text{B}2)_8]\text{O}_{30}$. Another layered structure like bismuth titanate ($\text{Bi}_4\text{Ti}_3\text{O}_{12}$) is also known to have the ferroelectric characteristics.[1-3]

Some investigations of composite materials based on two different crystal structures have been made.[4-7] However, these publications were oriented on development of dielectric device by making of flat dielectric curves with respect to temperature such as the case of X7R compositions. When composites composed of two different crystal structures are made, a transfer of matters between the two structures will occur. However, systematic study of the phase development and sintering behavior and on change of electrical characteristics has not been conducted so far.

In this work, the ferroelectric composites of perovskite structured BaTiO_3 (BT) and tungsten bronze structured $\text{Ba}_2\text{NaNb}_5\text{O}_{15}$ (BNN) were considered as a model system. A point of similarity between perovskite

and tungsten bronze is that the framework of these structures is composed by oxygen octahedrons. In perovskites, only tetragonal tunnels, which are called A sites, are formed in the structure. In the tungsten bronze structure, various kinds of tetragonal, pentagonal and trigonal tunnels are formed and they are called A1, A2 and C site, respectively. In the case of stoichiometric BNN, Nb and Ba occupy B and A2 sites respectively, and Na occupies A1 sites, since the Na ion radius is smaller than that of Ba. Therefore, BNN is called as filled tungsten bronze structure because every A and B sites are completely filled.

In this study, the ferroelectric ceramic composites of BNN and BT were prepared. The phase development and sintering behavior as well as dielectric characteristics of obtained materials were examined as a function of the molar ratio x in $(1-x)\text{Ba}_2\text{NaNb}_5\text{O}_{15}-x\text{BaTiO}_3$.

EXPERIMENTAL

The starting powders of $(1-x)\text{Ba}_2\text{NaNb}_5\text{O}_{15}-x\text{BaTiO}_3$, where $x = 0.0-1.0$, were prepared using high purity raw materials of BaCO_3 (Kojundo Chem. Lab., Co. Ltd., Japan, 99.95%), Na_2CO_3 (Aldrich Chem., USA, 99.5%),

Paper presented at the conference Solid State Chemistry 2004, Prague, September 13 -17, 2004.

Nb₂O₅ (Kojundo Chem. Lab., Co. Ltd., Japan, 99.9%) and TiO₂ (Toho Titan Co., Japan, 99.9%) using the general solid state reaction process. In this work, the synthesis of the composites (1-*x*)BNN+*x*BT was carried out according to the two following methods. The first method is direct synthesis from raw materials, i.e., raw materials of BaCO₃, Na₂CO₃, Nb₂O₅ and TiO₂ were all mixed together and calcined then sintered. The second method is indirect synthesis, i.e., BNN and BT were synthesized separately and mixed together before sintering. No differences in experimental results between the two processing methods were observed. Therefore, we report the experimental procedure and the results conducted by the indirect synthesis method.

The composition of starting powders with different mol% of BaTiO₃ from *x* = 0.0 to *x* = 1.0 was weighed and wet mixed for 24 h in a plastic jar with zirconia balls and ethanol. After drying, the powder was calcined at 1200°C for 2 h, then ball milled again for 24 h for crushing. Green pellets of 10 mm diameter disks were cold isostatic pressed at a pressure of 100 MPa for 3 min. Samples were sintered at the temperature range of 1200 ~ 1350°C for 2 h with a heating rate of 5°C/min. The crystal structure and phase evolution were identified by an X-ray diffractometer (M03XHF, Mac Science, Japan) using Cu-K_α radiation. The density of sintered samples was determined by the Archimedes' method and the microstructure of polished samples was observed by using a scanning electron microscope (SEM; JEOL, JML5400, Tokyo, Japan). The average grain size in the sample was determined by linear intercept method [8] on the SEM photographs. An Ag electrode was screen-printed on the both surfaces of sintered specimens, and fired at 600°C for 10 min. Dielectric properties were analyzed by an impedance gain phase analyzer (HP4194A, U.S.A.) with a frequency increment on steps from 1 kHz to 1 MHz in the temperature range from -173 to 727°C at 2°C increments.

RESULTS AND DISCUSSION

Figure 1 shows the powder X-ray diffraction patterns of the samples sintered at 1250°C for 2 h. The typical diffraction spectrum of BNN phase was observed in the composition *x* = 0.0. When the content of BT increased to *x* = 0.4 in (1-*x*)BNN+*x*BT the shape of the diffraction patterns was not changed but the peaks were shifted to lower diffraction angle. While in the case of *x* = 0.6 perovskite BT phase started to appear and two phases of BT and BNN coexisted in the sample. In the case of *x* = 1.0, the typical diffraction pattern of the tetragonal BT phase was observed. Unlikely the case of adding BT to BNN, however, the case of adding BNN to BT showed two changes. The first change is that the

tetragonal BT transformed to Cubic phase at room temperature. As observed in figure 1, diffraction peaks at 45°, 50° and 56° were split with the (h k l) of (002) (200), (102) (210), (112) (211), respectively, at *x* = 1.0 composition, which are the typical appearance of tetragonal phase. While the peaks were not split below *x* = 0.95, signifying that the BT phase is cubic. The second change is the development of Ba₆Ti₇Nb₉O₄₂ second phase, [9] which observed in the range of *x* = 0.8~0.95. The density of Ba₆Ti₇Nb₉O₄₂ phase is about of 5.29 g/cm³ and its melting temperature is around of 1400°C. When *x* = 0.8, three phases of BT, BNN and Ba₆Ti₇Nb₉O₄₂ coexisted.

Figure 2 shows the lattice constants of BNN and BT as a function of the BNN/BT ratio. The variation of lattice constants of BNN with respect to the content of BT (*x*) is presented in figure 2a. Lattice constants *a* and *c* for pure BNN were 17.593 ± 0.004 and 7.970 ± 0.002 Å, respectively. When BT is added up to *x* = 0.6, the lattice constants *a* and *c* increased almost linearly to 17.632 ± 0.006 and 7.997 ± 0.004 Å, respectively. Further addition of BT up to *x* = 0.8 did not affect the value of lattice constants. On the basis of the phase development behavior shown in figure 1 and the lattice constants values, the solubility limit of BT in BNN is thought to exist between *x* = 0.4 and *x* = 0.6. During the solid solution of BT in BNN, in order to satisfy electrical neutrality, it is believed that the Ba²⁺-Ti⁴⁺ pair of BT substitutes for Na⁺-Nb⁵⁺ pair of BNN. Because the ionic radius of Ti⁴⁺ (0.61 Å at CN = 6) is smaller than that of Nb⁵⁺ (0.64 Å at CN = 6) and the ionic radius of Ba²⁺ (1.60 Å at CN = 12) is larger than that of Na⁺ (1.39 Å at CN = 12), it is expected that the ions substitute for the A site have more influence on lattice constants than the ions does to

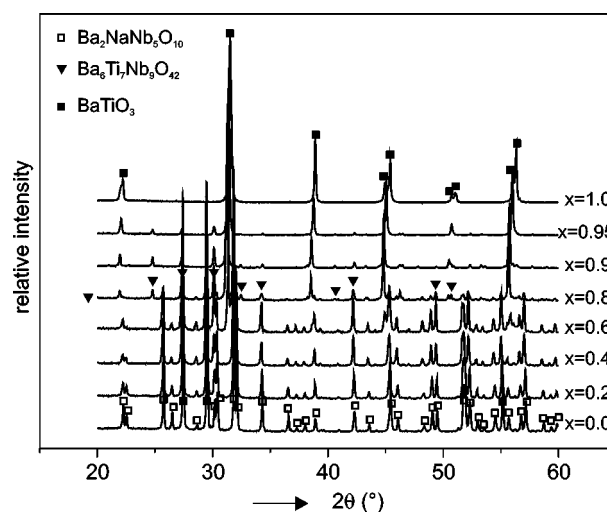
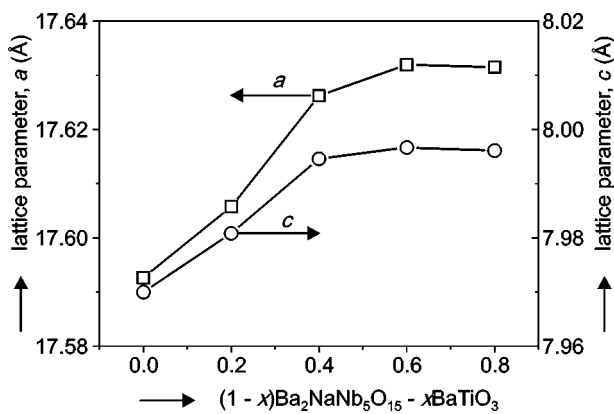
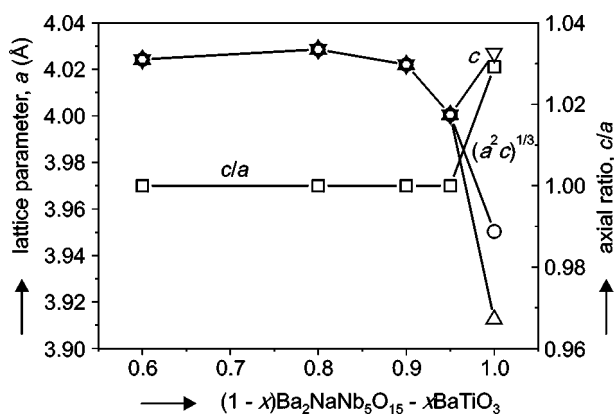


Figure 1. X-ray diffraction patterns of BNN-BT samples sintered at 1250°C for 2 h with different *x* in (1-*x*)BNN-*x*BT.

B sites when BT is added to BNN. In BNN-BT composites, it is thought that the solubility of BT is limited due to the difference in crystal structure between BT and BNN. In the case of one by one substitution between $Ba^{2+}-Ti^{4+}$ and Na^+-Nb^{5+} pairs in BNN, the number of A1 sites occupied by Na is smaller than the number of sites occupied by any other cations since there are two A1, four A2 and ten B sites in the BNN tungsten bronze formula. Because the cation ratio A/B of BNN and BT is 6/10 and 1/1 ($=10/10$), respectively, there would be no $Ba^{2+}-Ti^{4+}$ pairs soluble in BNN when every Na ions in two A1 site of BNN are substituted by Ba in BT. Therefore, the solubility limit of BT is expected to be the point when $Ba_2NaNb_5O_{15}$ (BNN) transforms to $Ba_3TiNb_4O_{15}$. [10] $x = 0.5$ will be the theoretical point of the solubility limit and the lattice constants shown in figure 2a agree with the theoretical value. On the other hand, even though the detail experimental results are



a)



b)

Figure 2. Variation of (a) tungsten bronze lattice parameters (a and c) and (b) perovskite lattice parameters (a , c and $(a^2c)^{1/3}$), tetragonality factors (c/a) of the samples sintered at 1250°C for 2 h as a function of x in $(1-x)\text{BNN}-x\text{BT}$.

not presented here, some extent of weight loss after sintering was observed and the weight loss increased from 0.4 % to 0.7 % as x increased from $x = 0.0$ to $x = 0.6$. Among the expelled Na and Nb ions due to the Ba and Ti substitutions, Na ions could be easily evaporated, which seems to be the result of the weight loss after sintering.

On the contrary to the case of BT addition to BNN, Na^+-Nb^{5+} pair of BNN will substitute for $Ba^{2+}-Ti^{4+}$ pair of BT as BNN is added to BT. In this case, according to our calculation, the perovskite structure became unstable due to the great decrease in tolerance factor,[11] and resulted in the formation of $Ba_6Ti_7Nb_9O_{42}$ second phase as shown in figure 3. From this point of view, in the case of BT addition to BNN, it is understandable that most of the expelled Na^+-Nb^{5+} pair is not soluble in BT and remain in the sample. When small amount of BNN is added, the perovskite BT changed to cubic structure in room temperature, and the mean lattice constant $(a^2c)^{1/3}$ increased from $3.950 \pm 0.004 \text{ \AA}$ ($x = 1.0$) to $4.022 \pm 0.003 \text{ \AA}$ ($x = 0.9$). More addition of BNN to $x = 0.6$ kept the lattice constant almost invariant around $4.024 \pm 0.005 \text{ \AA}$.

Figure 3 shows the relative volume fractions of BNN, BT and $Ba_6Ti_7Nb_9O_{42}$ which were obtained from the respective integrated x-ray intensities of the major peaks of each phase. This system can be divided into three regions from the phase development behavior. Region I is the area of $x = 0.0\sim 0.4$, showing a wide range of solid solution of BT in BNN. Region III, where the second phase of $Ba_6Ti_7Nb_9O_{42}$ is developed in BT, corresponds to $x = 0.9\sim 1.0$. Region II is in the area between region I and III, ranging $x = 0.6\sim 0.8$, which contains BNN, BT and the $Ba_6Ti_7Nb_9O_{42}$ second phase.

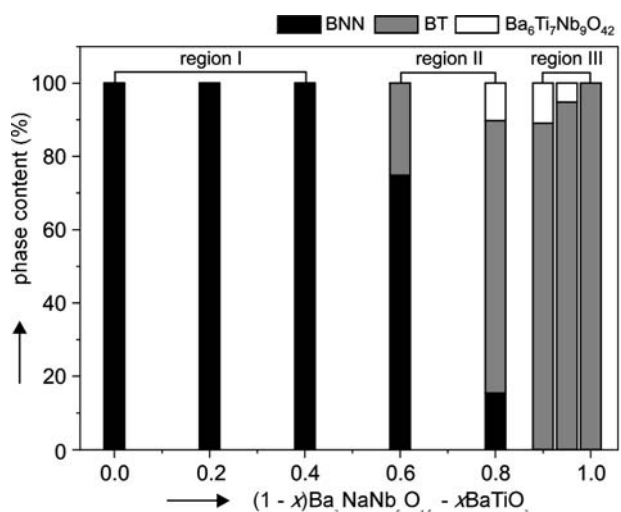


Figure 3. Variation of the BNN, BT and $Ba_6Ti_7Nb_9O_{42}$ phase content of the samples sintered at 1250°C for 2 h as a function of x in $(1-x)\text{BNN}-x\text{BT}$.

Figure 4 shows the bulk density of samples as functions of sintering temperature and BNN/BT ratio. The samples were sintered at various temperatures for 2 h. In the case of pure BNN ($x = 0.0$) in region I, densities of sintered body continuously increased as the sintering temperature increased up to 1350°C. When small amount of BT ($x = 0.2$) is added to BNN the densification was promoted at low temperature. However, when $x = 0.4$, the density of the sample sintered at 1300°C was lower of the density of the sample sintered at 1250°C and the over firing phenomena was observed. In the case of pure BT ($x = 1.0$), the maximum densification was observed at 1350°C. In the case of the samples with $x = 0.95$ and $x = 0.9$ in region III, the temperature where the maximum density was obtained decreased down to 1300°C. In the case of samples in region II ($x = 0.6\sim 0.9$), densification was improved at low temperature compared to the case of region I and region III. However, the temperature where the maximum density was obtained decreased to 1250°C.

Figure 5 shows microstructure of the samples sintered at 1300°C for 2 h as a function of BNN/BT ratio. As shown in figure 5a, pure BNN ($x = 0.0$) revealed 2 μm of mean grain size and 87 % of apparent density. Low densification of pure BNN thought to be caused by the fact that BNN has filled tungsten bronze structure and ionic diffusion in the structure is not easier in comparison with other tungsten bronze structures containing empty sites.[12] When BT is added to BNN ($x = 0.2\sim 0.4$), abnormal grain growth was appeared as shown in figure 5b and c. Among the expelled $\text{Na}^+\text{-Nb}^{5+}$ pair in BT added BNN, some of the Na ions might be evaporated and other Na ions produced Na-rich second phase of which melting temperature is low.[13] The generation of the abnormal grain growth is probably due to a liquid phase originated from the second phase.

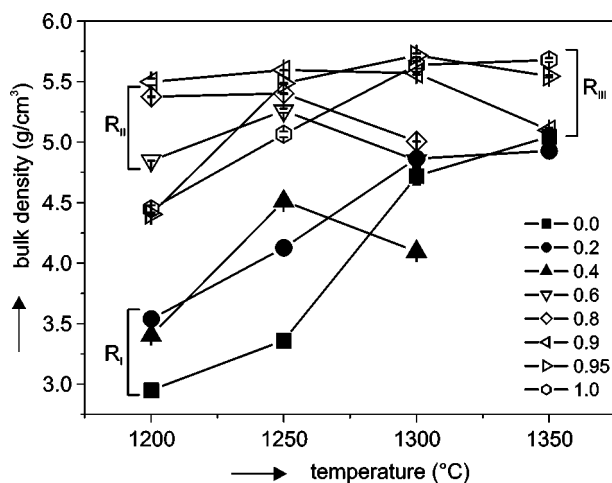
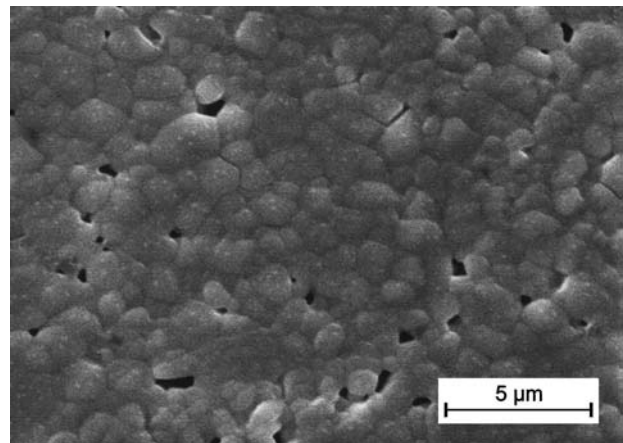


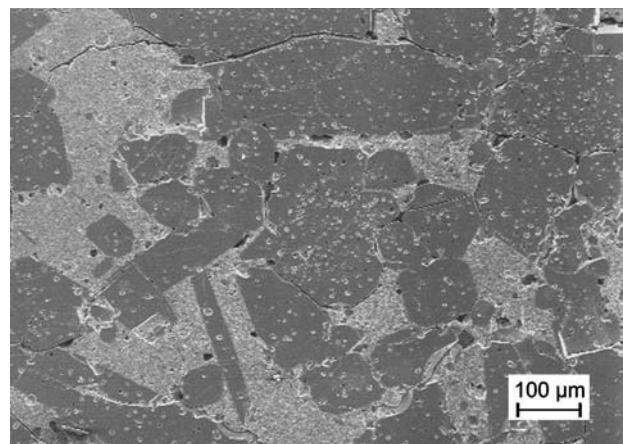
Figure 4. Bulk density of BNN-BT samples as function of sintering temperature and x in $(1-x)\text{BNN-xBT}$.

In the case of $x = 0.6\sim 0.8$ in region II shown in figure 5d and e, abnormal grain growth was inhibited and densification was promoted due to the pinning effect of $\text{Ba}_6\text{Ti}_7\text{Nb}_9\text{O}_{42}$ and BT phases in the BNN matrix. Pure BT in region III revealed the mean grain size of 7~8 μm and the apparent density of 89% as shown in figure 5f. When small amount of BNN was added to BT ($x = 0.9\sim 0.95$), densification was also improved by inhibiting the abnormal grain growth owing to the $\text{Ba}_6\text{Ti}_7\text{Nb}_9\text{O}_{42}$ second phase.

Figure 6 shows temperature dependence of dielectric constant of samples as a function of BT content in BNN. The Curie temperature (T_c) and the maximum dielectric constant (ϵ_{max}) at the Curie temperature of pure BNN ($x = 0.0$) revealed 540 and 1100°C, respectively, while Pure BT showed T_c of 112°C and max of 14600. The T_c decreased as the content of BT increased in the range of $x = 0.0\sim 0.6$. In the case of $x = 0.6$, two dielectric relaxation peaks were observed at 142°C and

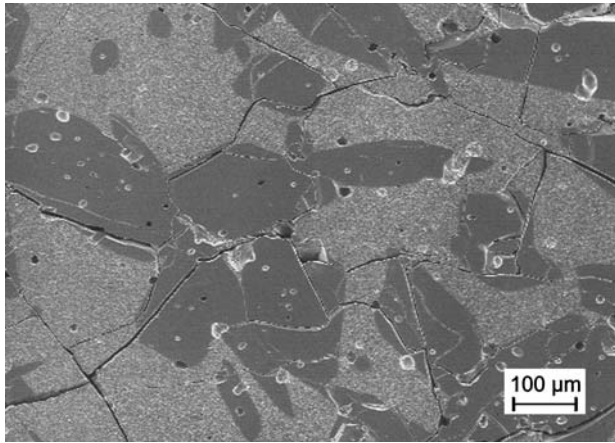


a)

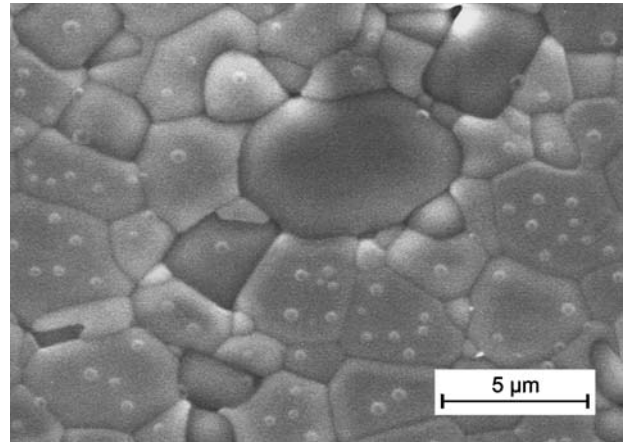


b)

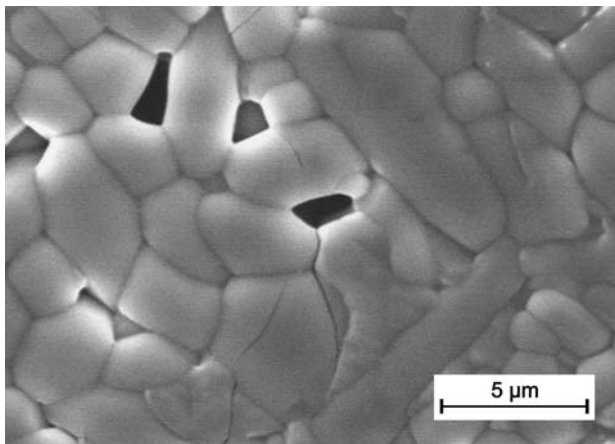
Figure 5. SEM photographs of BNN-BT samples sintered at 1300°C for 2 h with different x in $(1-x)\text{BNN-xBT}$. (a) $x = 0.0$, (b) $x = 0.2$.



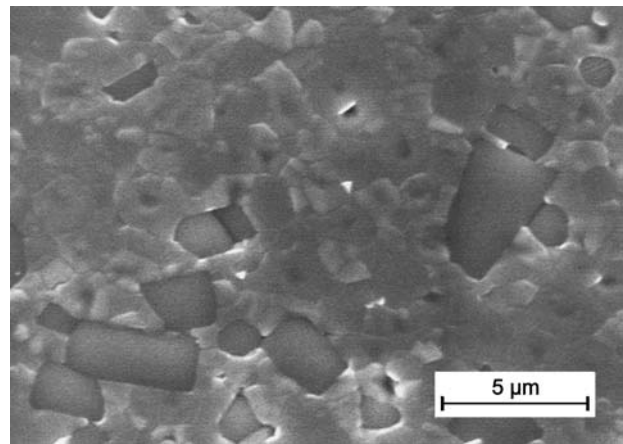
c)



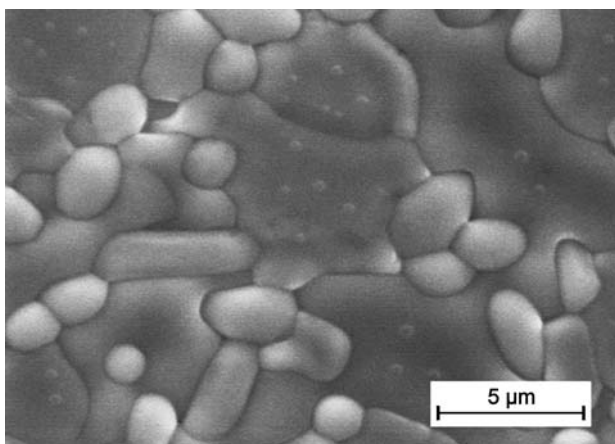
f)



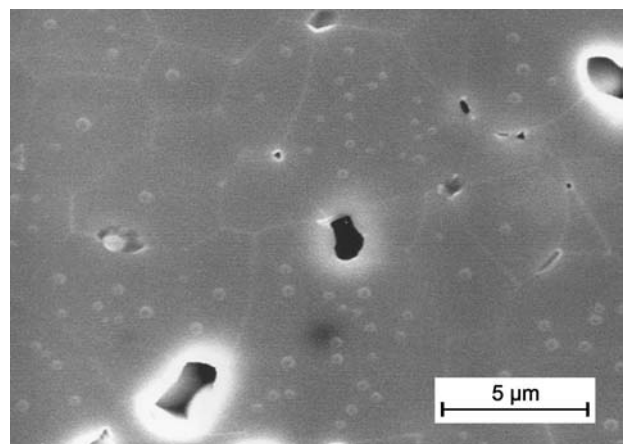
d)



g)



e)



h)

Figure 5. (continue) SEM photographs of BNN-BT samples sintered at 1300°C for 2 h with different x in $(1-x)BNN-xBT$. (c) $x = 0.4$ (d) $x = 0.6$, (e) $x = 0.8$, (f) $x = 0.9$, (g) $x = 0.95$ and (h) $x = 1.0$.

-40°C and the peaks are thought to be originated from the tungsten bronze structured BNN and perovskite BT, respectively, because BNN and BT coexists in the sample. When BNN is added to BT in the range of $x = 0.6\text{--}0.95$, the T_C of the BT-rich composites did not changed significantly. Moreover, the second phase of $\text{Ba}_6\text{Ti}_7\text{Nb}_9\text{O}_{42}$ observed in the BT-rich composites is considered to have paraelectric characteristics which might not greatly affect the dielectric characteristics of the composites.

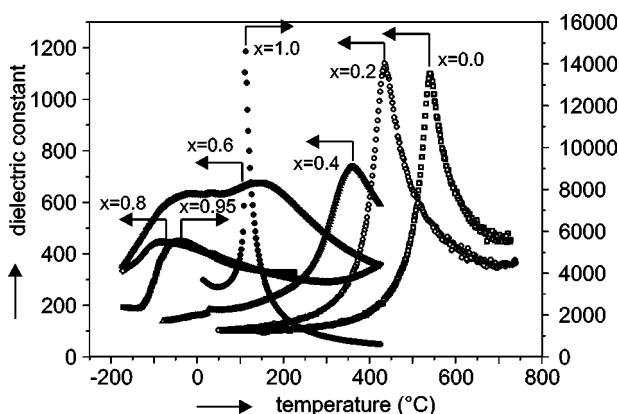


Figure 6. A comparison of dielectric constant of samples sintered at 1300°C for 2 h measured at 100 kHz with different x in $(1-x)\text{BNN}\cdot x\text{BT}$.

CONCLUSIONS

A wide range of solid solution of $(1-x)\text{Ba}_2\text{NaNb}_5\text{O}_{15}\cdot x\text{BaTiO}_3$ can be formed in the investigated system up to $x = 0.4\text{--}0.6$. The lattice constants increased with BT contents. Since the solid solution of BT extracts Na ions from BNN, a liquid phase might be produced containing the excess Na during the sintering and resulted in the abnormal grain growth. The BT contents over the solubility limit produced the second phase of $\text{Ba}_6\text{Ti}_7\text{Nb}_9\text{O}_{40}$ together with BT which played a role of grain growth inhibitor. The addition of BT to BNN shifted the T_C to lower temperature. The solubility limit of BNN in BT was very narrow comparing to the case of BT addition to BNN, which resulted in the generation of the second phase. The T_C of BT decreased suddenly when BNN is added. In the case of $x = 0.6$, two dielectric relaxation peaks were observed each of which is originated from BNN and BT phase, respectively.

Acknowledgement

This work was supported by grants No. R01-2003-000-11606-0 from the Basic Research Program of the Korea Science & Engineering Foundation.

References

- Xu Y.: *Ferroelectric Materials and Their Applications*, Elsevier Science Publishers, North-Holland 1991.
- Lines M. E., Glass A. M.: *Principles and Applications of Ferroelectrics and Related Materials*, Clarendon Press, Oxford 1984.
- Smolenskii G. A., Bokov V. A., Isupov V. A., Krainik N. N., Pasyukov R. E., Sokolov A. I.: *Ferroelectrics and Related Materials*, Gordon and Breach Science Publishers, 1984.
- Tribotte B., Desgardin G.: *Mater.Sci.Eng.B-Solid State Mater.Adv.Technol.* 40, 127 (1996).
- Chen R., Wang X., Li L., Gui Z. in: *Proceedings of the IEEE International Symposium on Applications of Ferroelectrics*, p.251-254, Ed. White G., Tsurumi T., Institute of Electrical and Electronics Engineers, New York 2002.
- Boufrou B., Desgardin G., Raveau B.: *J.Am.Ceram.Soc.* 74, 2809 (1991)
- Tribotte B., Hervieu M., Desgardin G.: *J.Mater.Sci.* 33, 4609 (1998)
- Fullmann R. L.: *Trans. AIME* 3, 447 (1953).
- Fang L., Zhang H., Qing L., Wu B.: *J.Wuhan Univ. Technol.-Mat.Sci.Edit.* 13, 42 (1998).
- Stephenson N.C.: *Acta Cryst.* 18, 496 (1965).
- Goldschmidt V. M.: *Shrifter Norske Videnskaps-Akad, Oslo I; Matemat, Naturvid, Klasse* (1929).
- Wang P., Lee J. H., Kim J. J., Cho S. H., Lee H. Y.: *Int.J.Mod. Phys.B* 17, 1273 (2003).
- Shafer M. W., Roy R.: *J.Am.Ceram.Soc.* 42, 485 (1959).

VÝVOJ MIKROSTRUKTURY A ELEKTRICKÝCH VLASTNOSTÍ KOMPOZITŮ $\text{Ba}_2\text{NaNb}_5\text{O}_{15}$ A BaTiO_3

MYOUNG-SUP KIM, JOON-HYUNG LEE, JEONG-JOO KIM, HEE YOUNG LEE*, SANG-HEE CHO

*Department of Inorganic Materials Engineering
Kyungpook National University, Daegu 702-701, Korea
*Department of Materials Science and Engineering
Yeungnam University, Gyeongsan 712-749, Korea*

Vývoj fázového složení, slinování a dielektrických vlastností kompozitů $\text{Ba}_2\text{NaNb}_5\text{O}_{15}$ (BNN) se strukturou wolframových bronzů a BaTiO_3 (BT) se strukturou perovskitu jsme zkoumali v řadě $(1-x)\text{Ba}_2\text{NaNb}_5\text{O}_{15}\cdot x\text{BaTiO}_3$. Až do $x = 0.4\text{--}0.6$ jsme zjistili široké rozmezí existence tuhých roztoků BT v BNN, přičemž velikosti mřížky rostly s rostoucím obsahem BT. Protože tuhý roztok BT vytěsňuje ionty Na z BNN, přebytečný Na může během slinování tvořit kapalnou fázi a tím urychlovat zhutňování a abnormální růst krystalů. Přídavek BT převyšující jeho rozpustnost v BNN vede ke tvorbě další fáze, $\text{Ba}_6\text{Ti}_7\text{Nb}_9\text{O}_{40}$, společně s BT, a tato fáze hraje hlavní roli inhibitoru růstu krystalů. Curieova teplota (T_C) a nejvyšší dielektrická konstanta BNN klesá s rostoucím obsahem BT. Navíc, je-li BNN přidán k BT, hranice rozpustnosti BNN v BT je velmi úzká ve srovnání s přidáním BT k BNN, který vede ke tvorbě druhé fáze $\text{Ba}_6\text{Ti}_7\text{Nb}_9\text{O}_{40}$. Přídavek BT k BNN rovněž posunuje T_C k nižším teplotám. Při $x = 0.6$ jsme pozorovali dva dielektrické relaxační píky, o nichž se domníváme, že jejich důvodem je koexistence BNN a BT ve vzorku.